ELSEVIER

www.elsevier.nl/locate/jelechem

Journal of Electroanalytical Chemistry 483 (2000) 68–80

Journal of Electroanalytical Chemistry

Capillary waves at soft electrified interfaces[☆]

L.I. Daikhin [a], A.A. Kornyshev [b], M. Urbakh [a,b,*]

[a] School of Chemistry, Tel Aviv University, Ramat Aviv, 69978 Tel Aviv, Israel
[b] Institute for Materials and Processes in Energy Systems, Research Center 'Jülich', 52425 Jülich, Germany

Received 15 November 1999; received in revised form 26 January 2000; accepted 2 February 2000

Abstract

Recent theory of capillary waves along the interface between two immiscible electrolytes is generalized to include the non-linear polarization of the double layer. The theory covers both the effects of the capillary waves on the double layer capacitance, as well as the effect of charging the interface on the amplitudes and spectrum of capillary waves. The theory explains major available experimental data, such as the interfacial capacitance dependence on the potential drop across the interface and on ionic strength. It also predicts a number of new effects, such as the influence of electric field and electrolyte concentration on the surface corrugation correlation function, and in particular, on the mean square height of corrugation. © 2000 Elsevier Science S.A. All rights reserved.

Keywords: Immiscible electrolyte solutions; Capillary waves; Double layer; Capacitance; Poisson–Boltzmann equation; Interfacial tension

1. Introduction

Electrochemistry of soft interfaces is a interdisciplinary field emerging rapidly, where soft matter physics [1] and physical chemistry of liquids [2] meet molecular electrochemistry [3]. One of the basic, proving-ground systems of soft matter electrochemistry is the interface of two immiscible electrolytes, a biomimetic system and model system for reaction-kinetics, but also a medium for the phase transfer catalysis [4,5] of industrial importance. One of the solvents is usually water, and the other one is a low polar organic liquid. This interface separates hydrophilic and hydrophobic ions. When two salts are dissolved in this system, one composed of hydrophobic and the other one of hydrophilic ions, they form two back-to-back electrical double layers and the interface can be polarized [4,5]. The resulting electric field across the interface affects a variety of phenomena, which occur at the interface.

First models of liquid | liquid interfaces in electrochemistry treated them as flat and sharp [4,5]. However, they are known to be never ideally flat because of the thermal excitation of capillary waves [6]. The interface itself, depending on the surface tension between the two liquids and some, even limited, penetration of hydrophobic ions in water and hydrophilic ions into the organic phase, may occur to be diffuse, looking rather as an interphase [7–9]. The overlapping of the two space charge regions influences essentially, the double layer capacitance. The two effects, diffuseness and capillary waves, are generally not unrelated. The effect of the short wavelength capillary waves leads to a creation of local protrusions at the interface which is hard to distinguish from that of diffuseness. Capillary wave theories usually result in the following expression for the effective width, d, of the liquid | liquid interface [6,10,11]:

$$d^2 = d_0^2 + d_{\mathrm{cw}}^2 \tag{1}$$

where d_0 and d_{cw} are the intrinsic (diffuseness) and capillary contributions to the surface width, respectively. A complete treatment of this problem requires a fully atomistic description of both the liquids and electrolytes, amenable to molecular dynamics computer simulations [12,13] and, in principle, to approximate

---

[☆] Paper presented at the Euroconference on Modern Trends in Electrochemistry of Molecular Interfaces, Finland, 28 August–3 September, 1999.

* Corresponding author. Tel.: +972-3-6408324; fax: +972-3-6409293.

E-mail address: urbakh@post.tau.ac.il (M. Urbakh)

PII: S0022-0728(00)00054-1

kinetic molecular theories of liquids [6]. There is also a possibility to separate these two contributions measuring an angular dependence of the X-ray reflectivity [14].

Effects of corrugation on electrical properties of the interface and on charge transfer phenomena across or near the interface, attracts considerable attention [5,12–15]. The electric field, a driving force of many phenomena at the interface, also affects this corrugation. Though it has never been shown experimentally, for the interface between two immiscible electrolytes, the studies of liquid helium films [16], and the surface of liquid metals [17–19] revealed strong enhancement of interfacial corrugation by an external electric field, up to a field induced destruction of the interface [20–23].

This article reports on the progress in the theory of capillary waves along a *sharp* interface of two *strictly* immiscible electrolytes and the effect of capillary waves on the electrical properties of the interface. The above mentioned system is a certain idealization of reality, even for an interface with large surface tension. However, this is the way to obtain the reference knowledge about the pure effect of capillary waves, before taking into account solvent and electrolyte interpenetration in the interfacial region.

2. Capillary waves along the interface of two immiscible liquids

Experiments on optical [24,25] and neutron reflectivity [26] and molecular dynamics simulations [12,13] unambiguously show that the liquid | liquid interface is highly corrugated. The corrugation originates from the thermal fluctuations of the interface, which are known as capillary waves. These fluctuations can be defined in terms of the dependence of the local height of the interface, z, on the lateral coordinate $\boldsymbol{R} = (x, y)$, given by the equation $z = \xi(\boldsymbol{R})$. The local height is determined versus the reference plane, $z = 0$, giving the zero average value of the profile function along this surface ($<\xi(\boldsymbol{R})> = 0$).

The spectrum of capillary waves can be calculated using the functional of the free energy of two contacting liquids

$$F = F_0 + F_{\mathrm{cw}}(\xi(\boldsymbol{R})) \tag{2}$$

where F_0 is the free energy of the system with a flat uncharged interface, while the second term stands for the energy excess due to surface corrugation:

$$F_{\mathrm{cw}}[\xi(\boldsymbol{R})] = 1/2 \int \mathrm{d}\boldsymbol{R}\gamma[(\nabla\xi(\boldsymbol{R}))^2 + k_{\mathrm{gr}}^2\xi^2(\boldsymbol{R})] \tag{3}$$

Here γ is the interfacial surface tension, k_{gr}^2 is the small wave-vector gravitational cutoff given by $\Delta\rho g/\gamma$, where g is the gravitational acceleration and $\Delta\rho > 0$ is the difference of the densities of two liquids.

The free energy functional is simplified after transformation to Fourier coordinates defined as

$$\xi(\boldsymbol{k}) = \int \mathrm{d}\boldsymbol{R}\xi(\boldsymbol{R}) \exp[-\mathrm{i}\boldsymbol{kR}] \tag{4}$$

Then we have

$$F_{\mathrm{cw}}[\xi(\boldsymbol{k})] = \frac{\gamma}{2} \int \frac{\mathrm{d}\boldsymbol{k}}{(2\pi)^2}\xi(\boldsymbol{k})\xi(-\boldsymbol{k})(k^2 + k_{\mathrm{gr}}^2) \tag{5}$$

Now the free energy is a quadratic functional of the fluctuating variable $\xi(k)$ and its treatment is trivial [27]. For the Fourier transform of the height–height correlation function

$$g(\boldsymbol{k}) = \int \mathrm{d}^2\boldsymbol{R}\langle\xi(\boldsymbol{R})\xi(0)\rangle \exp(-\mathrm{i}\boldsymbol{kR}) \tag{6}$$

due to the equipartition theorem [27] one obtains

$$g(\boldsymbol{k}) = \frac{k_{\mathrm{B}}T}{\gamma(k^2 + k_{\mathrm{gr}}^2)} \tag{7}$$

Here T is the absolute temperature, and k_{B} is the Boltzmann constant.

The mean square height of roughness, i.e. the capillary wave contribution to the width of the interface is expressed through the correlation function as

$$d_{\mathrm{cw}}^2 = \frac{1}{2\pi}\int_0^{k_{\max}} \mathrm{d}kkg(\boldsymbol{k}) \tag{8}$$

For $g(k)$ given by Eq. (7),

$$d_{\mathrm{cw}}^2 = \frac{k_{\mathrm{B}}T}{2\pi\gamma} \ln\left(\frac{k_{\max}}{k_{\mathrm{gr}}}\right) \tag{8a}$$

The upper wave-vector cutoff, $k_{\max}$, is introduced to eliminate the divergence of the integral, which takes place for $g(k)$ given by Eq. (7). Various estimates were proposed in the literature for $k_{\max}^{-1}$. It was assumed to be proportional to the root mean square height [11] or to the characteristic smearing of the interface [24], to the largest bulk correlation length of the contacting liquids [28]. In any case $\pi/k_{\max}$ cannot be less than the molecular diameter [29]. Gravity suppresses the long-range fluctuations and reduces a divergence of the correlation function at small wave vectors, $k < k_{\mathrm{gr}}$.

Both d_{cw} and $g(\boldsymbol{k}, V)$ can be measured in optical, neutron and X-ray scattering experiments [14,24–26], although it is more subtle to measure the height–height correlation spectrum than the integral characteristics of fluctuations, d_{cw}. Both experiments and molecular dynamics simulations [12–14,24–26] show that the macroscopic capillary wave theory works surprisingly well, down to the nanometer range.

Recent experiments on a time-resolved quasi-elastic laser scattering (QELS) [30,31] allowed us to measure the dispersion law of capillary waves, i.e. the relation between the frequency, ω, and their wavelength, $2\pi/k$. To derive the dispersion law theoretically, one must consider the dynamics of the two degrees of freedom: the dynamic position of the surface, $z = \xi(x, y, t)$, and the fluid velocity. In the limit of small viscosities, the capillary wave theory [6] gives

$$\omega^2 - 2\mathrm{i}\omega\Delta(k)^2 - \omega_c^2(k) = 0 \tag{9}$$

where

$$\omega_c^2(k) = \frac{k}{\rho_1 + \rho_2}\gamma(k^2 + k_{\mathrm{gr}}^2), \qquad \Delta(k) = 2k^2\frac{\eta_1 + \eta_2}{\rho_1 + \rho_2} \tag{10}$$

ρ_1, ρ_2 and η_1, η_2 are the densities and viscosities of contacting liquids. In contrast to neutron and X-ray scattering experiments [14,24–26], which allow us to study capillary fluctuations down to the nanometer scale, QELS measurements provide information on long wavelength fluctuations only, with wave lengths and frequencies of the order of 6.6×10^{-3}cm and 10 kHz, respectively [30,31].

3. Capillary waves along electrified interface between two immiscible electrolytes

Capillary waves at the interface of two immiscible electrolytes have been observed directly by a time-resolved quasi-elastic laser scattering [30,31], investigated in molecular dynamics computer simulations [12,13] and described within the framework of a *phenomenological theory* [32–34]. We summarize basic principles of this theory and discuss its results.

3.1. Equations to solve

The interface is described in the same way as in the previous section, using the approximation of smooth corrugations. The two electrolyte solutions are characterized by the solvent dielectric constants, ε_1 and ε_2, and Debye lengths, κ_1^{-1} and κ_2^{-1}. [For 1–1 binary electrolyte solutions $\kappa_i^{-1} = (\varepsilon_i k_B T/8\pi n_i^0 e^2)^{1/2}$, where n_i^0 is the bulk electrolyte concentration in the phase i (= 1, 2), and e is the charge of proton]. In addition to the *surface tension* term, the free energy functional now has two new terms. These are the *electrostatic energy*, F_e, and the term responsible for the *entropy of a dilute electrolyte*, F_s, i.e.

$$F = F_0 + F_{\mathrm{cw}}[\xi(\boldsymbol{R})] + F_e[\xi(\boldsymbol{R})] + F_s[\xi(\boldsymbol{R})] \tag{11}$$

where

$$\begin{aligned} F_e[\xi(\boldsymbol{R})] = &-\frac{\varepsilon_1}{8\pi}\int \mathrm{d}\boldsymbol{R}\int_{-\infty}^{\xi(\boldsymbol{R})}\mathrm{d}z[\nabla\varphi_1(z, \boldsymbol{R})]^2 \\ &+ e\int \mathrm{d}\boldsymbol{R}\int_{-\infty}^{\xi(\boldsymbol{R})}\mathrm{d}z\varphi_1(z, \boldsymbol{R})(n_1^+(z, \boldsymbol{R}) - n_1^-(z, \boldsymbol{R})) \\ &- \frac{\varepsilon_2}{8\pi}\int \mathrm{d}\boldsymbol{R}\int_{\xi(\boldsymbol{R})}^{\infty}\mathrm{d}z[\nabla\varphi_2(z, \boldsymbol{R})]^2 \\ &+ e\int \mathrm{d}\boldsymbol{R}\int_{-\infty}^{\xi(\boldsymbol{R})}\mathrm{d}z\varphi_2(z, \boldsymbol{R})(n_2^+(z, \boldsymbol{R}) - n_2^-(z, \boldsymbol{R})) + EQ \end{aligned} \tag{12}$$

and

$$\begin{aligned} F_s[\xi(\boldsymbol{R})] = k_B T\int \mathrm{d}\boldsymbol{R}\int_{-\infty}^{\xi(\boldsymbol{R})}\mathrm{d}z\Bigg[&n_1^+(z, \boldsymbol{R})\log\left(\frac{n_1^+(z, \boldsymbol{R})}{n_1^0}\right) \\ &+ n_1^-(z, \boldsymbol{R})\log\left(\frac{n_1^-(z, \boldsymbol{R})}{n_1^0}\right) - (n_1^+ + n_1^- + 2n_1^0)\Bigg] \\ + k_B T\int \mathrm{d}\boldsymbol{R}\int_{\xi(\boldsymbol{R})}^{\infty}\mathrm{d}z\Bigg[&n_2^+(z, \boldsymbol{R})\log\left(\frac{n_2^+(z, \boldsymbol{R})}{n_2^0}\right) \\ &+ n_2^-(z, \boldsymbol{R})\log\left(\frac{n_2^-(z, \boldsymbol{R})}{n_2^0}\right) - (n_2^+ + n_2^- + 2n_2^0)\Bigg] \end{aligned} \tag{13}$$

The notations used are as follows: $\phi_i(z, \boldsymbol{R})$ and $n_i^{\pm}(z, \boldsymbol{R})$ are the electrostatic potential and concentrations of positive and negative ions in the phase (i); E is the overall potential drop across the interface; Q and $-Q$ are the overall charges in the second and first phases, respectively.

The first term in Eq. (11), is again the free energy of the contacting solutions with a flat interface and with no charge in each of the double layers. The last term EQ in the expression for electrostatic energy is the extra work needed to maintain the overall potential difference E. This term should be included into the free energy functional when the overall potential drop between two phases is considered to be fixed [35].

This form of the functional implies a number of approximations. It assumes that the difference in the free energy of each ion transfer between water and the organic phase is so large that each sort of ion is either in water or in oil. A possible dipolar potential drop across the contact of the two liquids and its possible coupling with the ion distribution is not in the model.

The free energy functional depends on three types of fields: surface fluctuations $\xi(\boldsymbol{R})$, electrostatic potential $\phi_i(z, \boldsymbol{R})$, and the ionic concentrations $n_i^{\pm}(z, \boldsymbol{R})$. Minimizing the functional (Eq. (11)) with respect to ϕ_i and $n_i^{\pm}$ at a given $\xi(\boldsymbol{R})$, we obtain Poisson–Boltzmann equations, which describe the distribution of the electrostatic potential

$$\nabla^2\psi_1(z, R) = \kappa_1^2\sinh(\psi_1(z, R) - V) \quad \text{for } z < \xi(x, y) \tag{14}$$

$$\nabla^2\psi_2(z, R) = \kappa_2^2\sinh(\psi_2(z, R)) \quad \text{for } z > \xi(x, y) \tag{15}$$

and ionic concentrations

$$\begin{aligned} n_1^{\pm}(z, \boldsymbol{R}) &= n_1^0\exp[\mp(\psi_1(z, \boldsymbol{R}) - V)] \\ n_2^{\pm}(z, \boldsymbol{R}) &= n_2^0\exp[\mp\psi_2(z, \boldsymbol{R})] \end{aligned} \tag{16}$$

Here we introduced dimensionless potentials: $\psi_1 = e\beta\phi_1$, $\psi_2 = e\beta\phi_2$, $V = e\beta E$, where $\beta = (k_B T)^{-1}$.

The potential obeys standard boundary conditions at the interface:

1. continuity of potential:

$$\psi_1(x, y, z = \xi(x, y)) = \psi_2(x, y, z = \xi(x, y)) \tag{17}$$

2. the continuity of the normal component of electric induction:

$$\varepsilon_1 \frac{\partial\psi_1(\boldsymbol{R}, z = \xi(\boldsymbol{R}))}{\partial \boldsymbol{n}} = \varepsilon_2 \frac{\partial\psi_2(\boldsymbol{R}, z = \xi(\boldsymbol{R}))}{\partial \boldsymbol{n}} \tag{18}$$

   ($\partial/\partial\boldsymbol{n}$ denotes the gradient of the field along the normal to the interface);

3. the fixed value of the overall potential drop, V,

$$\psi_1 \to V \text{ as } z \to -\infty, \text{ and } \psi_2 \to 0 \text{ as } z \to \infty \tag{19}$$

It should be noted that Eqs. (14)–(16) have been derived under the assumption that the ionic subsystem is in equilibrium with respect to fluctuations of the interface. This assumption may be invalid for a high frequency domain of the capillary wave spectrum. Complications associated with the breakdown of this approximation will be discussed in Section 4.

3.2. Perturbation theory

The free energy functional can be essentially simplified if the amplitudes of capillary waves are small, i.e. if one assumes that for each Fourier-component of surface fluctuation $\xi(\boldsymbol{k})$ the inequality $|\xi(\boldsymbol{k})| < 2\pi/|\boldsymbol{k}|$ holds. Then (for details see Refs. [32,34])

$$F[\xi(\boldsymbol{k}), V] = F_0 - \frac{S}{2}V^2 C_{GC} + \Delta F[\xi(\boldsymbol{k}), V] \tag{20}$$

Here, S is the apparent (flat cross-section) interfacial area, C_{GC} is the Gouy–Chapman capacitance of two back-to-back ionic double layers separated by a flat interface [4],

$$\frac{1}{C_{GC}} = \frac{1}{C_1} + \frac{1}{C_2} \tag{21}$$

$$C_i = \frac{\varepsilon_i \kappa_i}{4\pi}\left[1 + \frac{4\pi^2\sigma_0^2}{(\varepsilon_i\kappa_i)^2}\right]^{(1/2)}, \quad i = 1, 2 \tag{22}$$

and σ_0 is the charge density in each double layer per unit area of a flat interface.

The first two terms in Eq. (20) present the free energy of the contacting solutions with a flat interface for a given potential drop V. The correction due to interfacial fluctuations is given by

$$\begin{aligned}\Delta F[\xi(\boldsymbol{k}), V] \\ = \frac{1}{2}\int \frac{\mathrm{d}\boldsymbol{k}}{(2\pi)^2}\xi(\boldsymbol{k})\xi(-\boldsymbol{k})\{\gamma(k^2 + k_{gr}^2) - \Delta f(k, V)\}\end{aligned} \tag{23}$$

The explicit expression for the potential dependent function $\Delta f(k, V)$ is cumbersome. It is shown here for the limit of high concentration of electrolyte in the aqueous phase (see Appendix A)

$$\begin{aligned}\Delta f(k, V) = {} & \frac{\kappa_2^3}{2\pi}\left(\frac{k_B T}{L_B^{(2)}}\right) \\ & \left\{ - f_1(k, V) + \frac{4\sinh\left(\frac{V}{2}\right)}{f_0(k, V)} f_2(k, V) \right. \\ & - \frac{2\sinh^2\left(\frac{V}{2}\right)}{f_0(k, V)}\left[\frac{k^2}{\kappa_2^2} + f_0(k, V)\cosh\left(\frac{V}{2}\right)\right] \\ & - V f_3(k, V) + 4\sinh^2\left(\frac{V}{2}\right)\cosh\left(\frac{V}{2}\right) \\ & \left. + V\sinh\left(\frac{V}{2}\right)\left[1 - \frac{k^2}{\kappa_2^2 f_0(k, V)}\right]\right\}\end{aligned} \tag{24}$$

where

$$L_B^{(2)} = \frac{e^2}{\varepsilon_2 k_B T}$$

is the Bjerrum length in the non-aqueous solution.

The functions $f_i(k, V)$, $i = 0, 1, 2, 3$ have the form

$$f_0(k, V) = \frac{q_2(k)}{\kappa_2} + \cosh\left(\frac{V}{2}\right)$$

$$f_1(k, V) = \sinh\left(\frac{V}{2}\right)[V\cosh(V) + 3\sinh(V)] \tag{26}$$

$$\begin{aligned}f_2(k, V) = {} & \sinh\left(\frac{V}{2}\right)\left[\frac{k^2}{\kappa_2^2} + f_0(k, V)\cosh\left(\frac{V}{2}\right)\right] \\ & + \frac{V}{2}\frac{q_2(k)}{\kappa_2}\left[\frac{k^2}{\kappa_2^2} + \cosh^2\left(\frac{V}{2}\right)\right] \\ & + \frac{V}{2}\left[\frac{q_2^2(k)}{\kappa_2^2}\cosh\left(\frac{V}{2}\right) - \frac{k^2}{\kappa_2^2} f_0(k, V)\right. \\ & \left. + \sinh^2\left(\frac{V}{2}\right)\left(\cosh\left(\frac{V}{2}\right) + f_0(k, V)\right)\right]\end{aligned} \tag{27}$$

$$\begin{aligned}& f_3(k, V) \\ & = \frac{\sinh(V)}{2 f_0(k, V)}\left[f_0(k, V)\left(2\frac{q_2(k)}{\kappa_2} - \cosh\left(\frac{V}{2}\right)\right)\right. \\ & \quad \left. + \sinh\left(\frac{V}{2}\right)\left(1 + \frac{k^2}{\kappa_2 q_2(k) f_0(k, V)}\right)\right] \\ & \quad + \frac{q_2(k)}{\kappa_2}\sinh^3\left(\frac{V}{2}\right) \\ & \quad \left[\frac{\kappa_2}{q_2(k)} + \cosh\left(\frac{V}{2}\right)\left(2 + 2\frac{\kappa_2}{q_2(k)}\cosh\left(\frac{V}{2}\right) + \frac{\kappa_2^2}{q_2^2(k)}\right)\right]\end{aligned} \tag{28}$$

where

$$q_2(k) = \sqrt{\kappa_2^2 + k^2}$$

Treating the functional $\Delta F[\xi(\boldsymbol{k}), V]$ as a Hamiltonian of the fluctuating variable $\xi(\boldsymbol{k})$ [26] and acting in the same way as in the derivation of Eq. (7), we find the potential dependent Fourier transform of the height–height correlation function

$$g(\boldsymbol{k}, V) = \frac{k_{\mathrm{B}}T}{\gamma[k^2 + k_{\mathrm{gr}}^2] - \Delta f(k, V)} \tag{29}$$

The mean square height of corrugation, d_{cw}^2, depends on the potential through $g(\boldsymbol{k}, V)$ via Eq. (8). The interface of two immiscible electrolytes gives rich possibilities to study these quantities, as one can vary the overall potential drop or electrolyte concentrations in both phases. It is certainly most challenging to verify Eq. (29) experimentally, but there is, however a conceptual problem with this equation. Indeed, the perturbation theory approach is justified rigorously only when $[g(k, V)]^{1/2}k \ll \pi$, but at large V the denominator of Eq. (29) may become small and this condition will not be fulfilled. Thus, one should not take Eq. (29) too literally, as it may exceed the accuracy of the approximations under which it was derived, although qualitatively, it should give the right trends. It may appear to work even quantitatively when the denominator is not too small.

Another experimentally accessible characteristic of the interface is the differential capacitance C, defined as

$$C = \mathrm{d}Q/\mathrm{d}E \tag{30}$$

The perturbation approach gives for the charge, Q, a cumbersome but fully closed form expression as a function of potential drop V. We give the one for the case of the full screening of the field in the aqueous phase (high electrolyte concentration) [36]

$$Q = \frac{e\kappa_2 S}{2\pi L_{\mathrm{B}}^{(2)}} \sinh\left(\frac{V}{2}\right)\left\{1 + \frac{1}{2}\int \frac{\mathrm{d}\boldsymbol{k}}{(2\pi)^2} k^2 g(\boldsymbol{k}, V) \left[1 - \frac{k^2}{\left(\kappa_2 \cosh\left(\frac{V}{2}\right) + q_2(k)\right)^2}\right]\right\} \tag{31}$$

Substituting Eq. (31) into Eq. (30) gives the following equation for the capacitance

$$C = C_{\mathrm{GC}}(V)\tilde{R}(\kappa_2, V) \tag{32}$$

where $\tilde{R}(\kappa_2, V)$, called the *roughness function*, reads

$$\tilde{R}(\kappa_2, V) = 1 + \frac{1}{4\pi}\int_0^{k_{\max}} \mathrm{d}k k^3 g(\boldsymbol{k}, V) \left[1 - k^2 \frac{\left(q_2(k) - \kappa_2 \cosh\left(\frac{V}{2}\right) + \frac{2\kappa_2}{\cosh\left(\frac{V}{2}\right)}\right)}{\left(\kappa_2 \cosh\left(\frac{V}{2}\right) + q^2(k)\right)^3}\right] + \tanh\left(\frac{V}{2}\right)\frac{1}{2\pi k_{\mathrm{B}}T}\int_0^{k_{\max}} \mathrm{d}k k^3 g^2(\boldsymbol{k}, V) \frac{\partial \Delta f(k, V)}{\partial V}\left[1 - \frac{k^2}{\left(\kappa_2 \cosh\left(\frac{V}{2}\right) + q^2(k)\right)^2}\right] \tag{33}$$

The Gouy–Chapman limit (Eqs. (21) and (22)) follows from this equation when $\gamma \to \infty$. The deviations from the Gouy–Chapman are accumulated in *the roughness function*. Note that the roughness function is determined not only by the correlation function, $g(\boldsymbol{k}, V)$, but also by its derivative with respect to the potential.

It should be noted that the above reservations concerning the limits of applicability of the perturbation theory remain valid for the capacitance too.

Recent experiments on the time-resolved quasi-elastic laser scattering [30,31] allowed us to measure the dispersion relation for the capillary waves at the interface between two immiscible electrolyte solutions. Our calculations demonstrate that charging of the interface modifies the dispersion law (Eq. (9)). It now reads,

$$\omega^2 - 2\mathrm{i}\omega\Delta(k) - \omega_c^2(k) + \frac{k}{\rho_1 + \rho_2}\Delta f(k, V) = 0 \tag{34}$$

i.e. charging the interface reduces the frequency of capillary waves. As we have already mentioned above, Eq. (34) gives a dispersion relation for long-wave length capillary fluctuations, which practically do not influence the capacitance. However, the field-induced correction to the dispersion relation is determined by the same function $\Delta f(k, V)$ as the corrections to the capacitance and to the height–height correlation function.

3.3. Low potential drop: linear response theory

If $V < k_{\mathrm{B}}T/e$, the distribution of the electrostatic potential $\psi(z, \boldsymbol{R})$ can be described by the *linearized* version of the Poisson–Boltzmann equations. To obtain the results, we still need the perturbation theory, but its algebra is much simpler. The linear response theory was reported in Refs. [32,33]. Due to relative simplicity of results, it has special tutorial value.

Note, that compact results are obtained here for *arbitrary* concentrations of electrolyte in *both* phases, and we present them as they are. However, when comparing them with those obtained for arbitrary V we will consider only the case of high concentrations in the aqueous phase.

The function $\Delta f(k, V)$, which determines the effect of charging on the interfacial corrugation, follows from the solutions of the *linearized* Eqs. (14) and (15):

$$\Delta f(k,V) = \frac{4\pi V^2 (C_{\mathrm{GC}}^{(0)})^2}{\varepsilon_1 q_1 + \varepsilon_2 q_2}[(q_2 - \kappa_2)(\varepsilon_1 q_1/\varepsilon_2 + \kappa_2) + (q_1 - \kappa_1)(\varepsilon_2 q_2/\varepsilon_1 + \kappa_1) - 2(q_1 - \kappa_1)(q_2 - \kappa_2)] \quad (35)$$

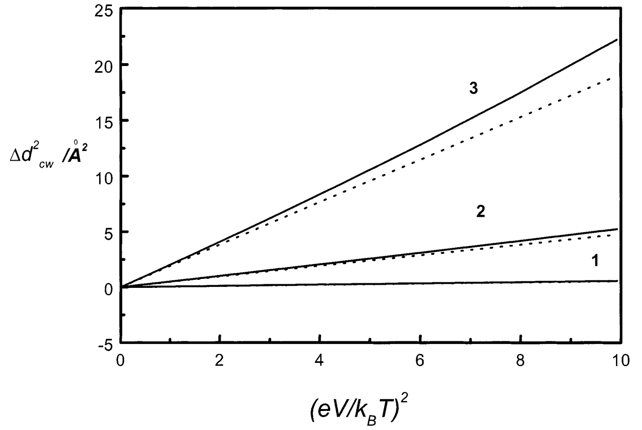

Fig. 1. The increase of the mean square height of corrugation, $\Delta d^2_{\mathrm{cw}} = d^2_{\mathrm{cw}} - (d^{(0)}_{\mathrm{cw}})^2$, versus the square of the potential drop. $\varepsilon_1 = 80$, $\varepsilon_2 = 10$, $k_{\mathrm{max}} = 2$ Å^{-1}, $k_{\mathrm{gr}} = 6 \times 10^{-8}$ Å^{-1} $n_1 = n_2 = 0.1$ M. The effect of interfacial tension at r.t. γ, dyn cm^{-1} = (1) 30, (2) 10, (3) 5. Solid lines present the results of calculations according Eqs. (8), (29) and (35), dotted lines show the assymtotic solution (Eq. (41)).

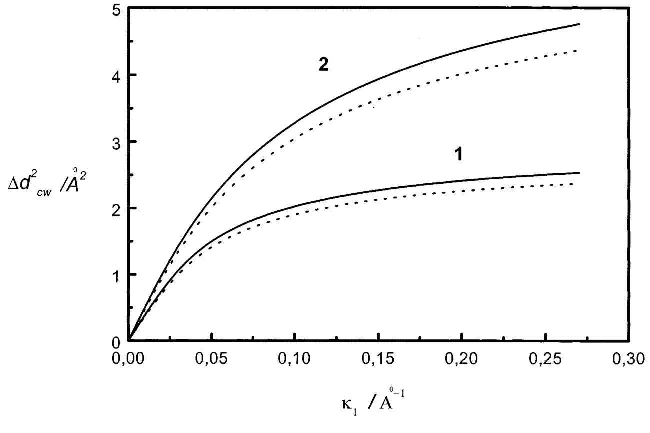

Fig. 2. The increase of the mean square height of corrugation, $\Delta d^2_{\mathrm{cw}} = d^2_{\mathrm{cw}} - (d^{(0)}_{\mathrm{cw}})^2$, versus the inverse Debye length in the aqueous phase, κ_1, at a fixed potential drop $eV = 2k_{\mathrm{B}}T$. $\varepsilon_1 = 80$, $\varepsilon_2 = 10$, $k_{\mathrm{max}} = 2$ Å^{-1}, $k_{\mathrm{gr}} = 6 \times 10^{-8}$ Å^{-1}, $\gamma = 30$ dyn cm^{-1}. The effect of the inverse Debye length in the non-aqueous phase κ_2/Å^{-1} = (1) 0.1, (2) 0.2. Solid lines present the results of calculations according Eqs. (8), (29) and (35), dotted lines show the asymtotic solution (Eq. (41)).

where $C^{(0)}_{\mathrm{GC}}$ is the Gouy–Chapman capacitance of the flat interface between two electrolyte solutions at the point of zero charge (pzc)

$$C^{(0)}_{\mathrm{GC}} = \frac{\varepsilon_1 \varepsilon_2 \kappa_1 \kappa_2}{4\pi(\varepsilon_1 \kappa_1 + \varepsilon_2 \kappa_2)} \quad (36)$$

and

$$q_1 \sqrt{\kappa_1^2 + k^2}, \qquad q_2 = \sqrt{\kappa_2^2 + k^2} \quad (37)$$

That results in the following asymptotic laws in the regions of small and large wave vectors:

$$\Delta f(k, V) \approx \frac{1}{2} k^2 V^2 C^{(0)}_{\mathrm{GC}} \quad \text{for} \quad k \ll \kappa_1, \kappa_2 \quad (38)$$

$$\Delta f(k, V) \approx 4\pi V^2 (C^{(0)}_{\mathrm{GC}})^2 k \frac{(\varepsilon_1 - \varepsilon_2)^2}{(\varepsilon_1 + \varepsilon_2)\varepsilon_1 \varepsilon_2} \quad \text{for} \quad k \gg \kappa_1, \kappa_2 \quad (39)$$

The substitution of Eq. (38) into Eq. (29) shows that for $k \ll \kappa_1$, κ_2, the electric field affects the corrugation merely via a decrease of the interfacial tension,

$$\gamma_{\mathrm{eff}} = \gamma - \frac{1}{2} V^2 C^{(0)}_{\mathrm{GC}} \quad (40)$$

That is in line with a standard thermodynamic result given by the Lippmann equation [37]. However, for larger wave-vectors the field-effect is not reduced to the reduction of γ; the dependence is more complicated.

The mean square height of interfacial corrugation follows from Eqs. (8), (29) and (35)

$$d^2_{\mathrm{cw}} \approx (d^{(0)}_{\mathrm{cw}})^2 + \frac{V^2 k_{\mathrm{B}} T}{4\pi\gamma^2} C^{(0)}_{\mathrm{GC}} \ln \frac{\kappa_1 \kappa_2}{(\kappa_1 + \kappa_2) k_{\mathrm{gr}}} \quad (41)$$

where $d^{(0)}_{\mathrm{cw}}$ is the root mean square height of the pzc. Eq. (41) shows directly that the charging of the interface leads to an enhancement of surface corrugation. Note, that the increase of d_{cw} relative to $d^{(0)}_{\mathrm{cw}}$ does not depend on the upper cut-off.

In Fig. 1 we show the linear response results for the dependence of the mean square height on the potential drop at a given (typical) electrolyte concentration and several values of the interfacial tensions. For low, but realistic surface tensions the effect is large enough even for moderate potential drops. The asymptotic expression (Eq. (41)) works fairly well in this region. Note that computer simulations for two contacting solvents (without electrolytes) in an external field show the V^2-law in a much wider range of potentials [13].

Fig. 2 shows the dependence of d^2_{cw}on electrolyte concentration for a given, moderate potential drop. The effect is larger the greater the electrolyte concentration. However, one should be careful in extending this conclusion to molar concentrations. It is well known that the mean field Poisson–Boltzmann theory may break down here, due to the effects of ion packing leading to the formation of crystal-like structures [38,39].

The linear response theory gives a simple expression for the capacitance

$$C = C^{(0)}_{\mathrm{GC}} \tilde{R}(\kappa_1, \kappa_2, V = 0) \tag{42}$$

where

$$\tilde{R}(\kappa_1, \kappa_2, V = 0) = 1 + 2C^{(0)}_{\mathrm{GC}} \int_0^{k_{\max}} \mathrm{d}k g(\boldsymbol{k}, V) = 0)$$

$$\frac{k}{\varepsilon_1 q_1 + \varepsilon_2 q_2} \{(q_1 - \kappa_1)[(\kappa_1 + \kappa_2) + q_2(\varepsilon_2 - \varepsilon_1)/\varepsilon_1] + (q_2 - \kappa_2)[(\kappa_1 + \kappa_2) + q_1(\varepsilon_1 - \varepsilon_2)/\varepsilon_2]\} \tag{43}$$

Thus, in order to calculate the differential capacitance at the pzc it is sufficient to know the correlation function of corrugation for $V = 0$, which is given by Eq. (7).

For $\gamma \to \infty$, Eq. (43) gives $\tilde{R}(\kappa_1, \kappa_2) = 1$ reproducing the Gouy–Chapman result for the capacitance of a flat interface. Eqs. (42) and (43) show that the double layer capacitance at the liquid | liquid interface increases with the amplitude of surface corrugation, and it is always larger than the one prescribed by Gouy–Chapman theory for a flat interface. The effect of corrugation on the double-layer capacitance is determined by an interplay between the Debye lengths in the two electrolytes, κ_1 and κ_2, and the scales of roughness [33]. As expected, Eq. (43) shows that for the small Debye lengths, κ_1^{-1} and $\kappa_2^{-1} \to 0$, the roughness function, $\tilde{R}(\kappa_1, \kappa_2)$, approaches the geometrical roughness factor R ($= S_{\mathrm{real}}/S$, i.e. the ratio of the true surface to the apparent surface). At very large Debye lengths, κ_1^{-1} or $\kappa_2^{-1} \to \infty$, the roughness of the interface is not seen in the capacitance and $\tilde{R} = 1$.

The equation, which is similar to Eq. (43) has been derived recently in Ref. [40]. The use of the non-local boundary condition suggested in Ref. [40] is equivalent to the procedure described in the present work. Actually, the additional non-local boundary condition [40] is not a boundary condition. It is a definition of the form of the approximation used for the potential distribution at the interface. This condition includes unknown functions which are determined by substituting it into the usual boundary conditions (Eqs. (17) and (18)). The results of this procedure are equivalent to the one described above.

Thus the difference in the approach of Ref. [40] and our approach (Refs. [32,33] and this paper) is NOT in different boundary conditions. The points of difference are as follows.

- The authors of Ref. [40] analyzed the equation for the capacitance assuming that an interfacial profile can be described by a sinusoidal function. However, the corrugation of liquid | liquid interfaces cannot be described by a single-sinusoidal profile function; there is a whole spectrum of harmonics that contribute to the capillary fluctuations [2,6]. In our work we have analyzed equations for the capacitance using height–height correlation functions (see Eqs. (7) and (29)) suggested by a standard capillary wave theory.
- The effect of electric field on the corrugation of liquid | liquid interfaces was not considered in Ref. [40]. Here we demonstrate that this effect gives a large contribution to the double layer capacitance at soft interfaces. We treat the effect of the electric field on capillary waves and the effect of capillary waves on the double layer capacitance in a self-consistent fashion.

Let us show the typical scale of the effect, first, using the traditional Parsons–Zobel plots. In Fig. 3 we vary the concentration of electrolyte in water (one of the contacting phases) keeping constant the concentration in the non-aqueous phase. Deviation from the Gouy–Chapman capacitance depends on the interfacial tension and dielectric constant of the non-aqueous medium. Changing the medium, we change both parameters simultaneously. For tutorial purposes, however, we show the effect of these two parameters separately. In accordance with experimental data [7,8,41–44] we see that the effect of capillary waves leads to an increase of the capacitance, relative to C_{GC}. The lower the dielectric constant of the non-aqueous medium, the stronger is the deviation (Fig. 3a). The reason for this effect is clear. The smaller dielectric constants will decrease the effective Debye length, $1/\kappa_1 + 1/\kappa_2$. The electric field then probes the Fourier components of fluctuations with higher wave vectors that give the largest contribution to the roughness function. The increase of the interfacial tension depresses the capillary waves (the mean square fluctuation scales as $1/\gamma$) and the deviation from the Gouy–Chapman result is smaller (Fig. 3b). The typical absolute values of the effect lie in the observed interval [7], but they strongly depend on the cutoff (Fig. 3c).

However, in the context of this problem, the Parsons–Zobel plots are rather featureless. Much more informative is to plot directly the *roughness function*, in which the effect of capillary waves is much better seen (Figs. 4 and 5). It is stronger, the larger the upper wave-vector cutoff (cf. (a) and (b)). Fig. 4 shows the roughness function variation with the inverse Debye length of the aqueous electrolyte for several fixed values of the ionic concentration in the non-aqueous phase. The effect of the dielectric constant of the non-aqueous phase is shown in Fig. 5 for a fixed electrolyte concentration in the non-aqueous phase.

We, thus, suggest treating the experimental data in terms of the roughness function, varying the concentrations of electrolytes. The theory predicts a definite shape of this function. If this shape were experimentally observed, one could fit the data with one adjustable

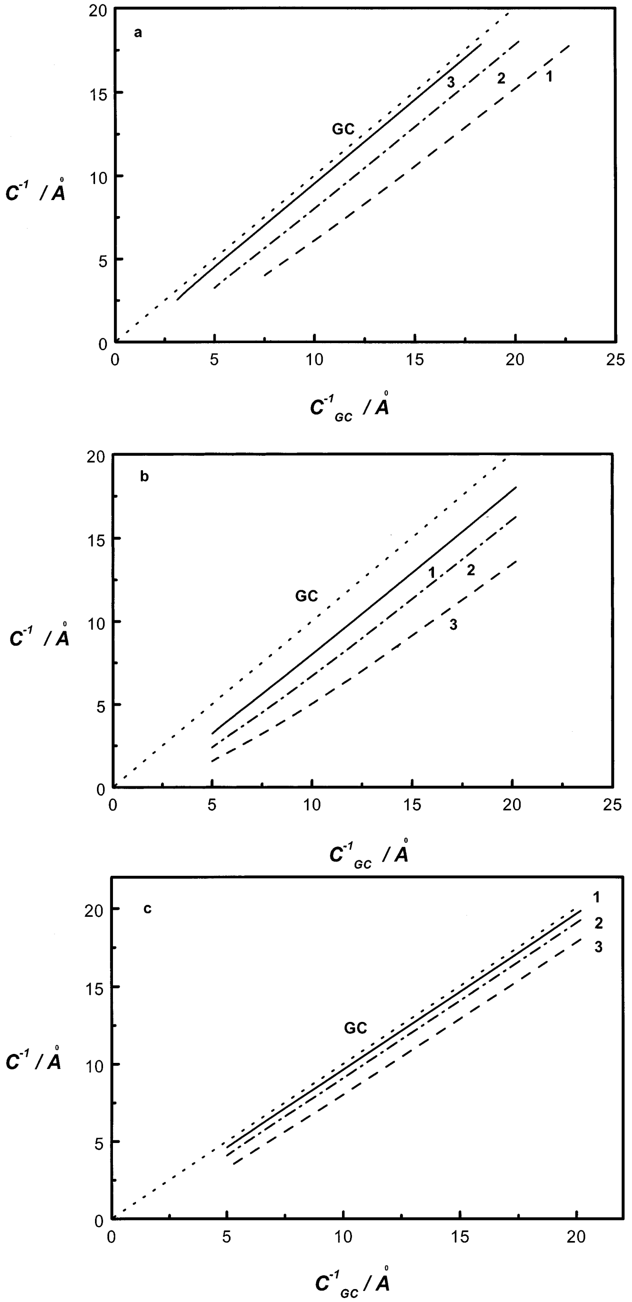

Fig. 3. Parsons–Zobel plots calculated by varying the concentration of electrolyte in water for a given concentration of electrolyte in the non-aqueous phase, $n_2 = 0.1$ M. Dotted line shows the Gouy–Chapman reference line. (a) $\gamma = 30$ dyn cm^{-1}, $k_{\max} = 2$ Å^{-1}. The effect of dielectric constant of the non-aqueous solvent. $\varepsilon_2 =$ (1) 4, (2) 10, (3) 30. (b) $\varepsilon_2 = 10$, $k_{\max} = 2$ Å^{-1}. The effect of interfacial tension at r.t. γ, dyn cm^{-1} = (1) 30, (2) 15, (3) 7.5. (c) $\gamma = 30$ dyn cm^{-1}, $\varepsilon_2 = 10$. The effect of the upper wave-vector cutoff $k_{\max}$/Å^{-1} = (1) 0.5, (2) 1, (3) 2.

parameter of the theory: the upper wave-vector cutoff, $k_{\max}$. The latter lies in the range of 2–0.5 Å^{-1} [10,12,45] and is a constant for the given pair of liquids in contact. Indeed, the concentration dependence of $k_{\max}$ should be negligible for low and moderate ionic strengths [6]. The same refers to γ.

3.4. Beyond the linear theory

The main drawbacks of the linear theory is that except for the case of very low interfacial tensions, remarkable deviations from the Gouy–Chapman theory take place at $V > k_BT/e$, i.e. beyond the limits of validity of the linear response theory. Thus, in general we should use the more cumbersome expressions of the non-linear theory. In Figs. 6–8 we show the predictions of the linear and non-linear theories.

Fig. 6a demonstrates the increase of the mean square height of corrugation with the potential drop across the interface for several fixed values of the electrolyte concentration in a non-aqueous solution. We found that d^2_{cw} grows dramatically when the potential approaches a critical potential, above which the interface becomes unstable under the influence of the strong electric field. For reasonable values of the interfacial tension and ionic concentrations the critical potential lies in the range of hundreds mV. For a given potential the enhancement of d^2_{cw} increases and a value of the critical

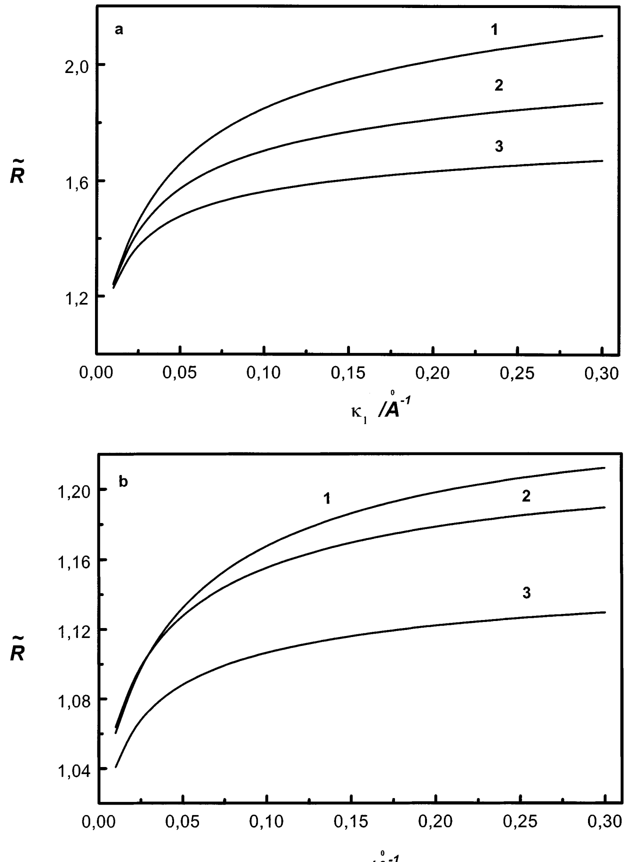

Fig. 4. Roughness function versus the Debye length in the aqueous phase at a fixed interfacial tension, $\gamma = 15$ dyn cm^{-1}, and a given dielectric constant of the non-aqueous solvent, $\varepsilon_2 = 10$. The upper wave-vector cutoff $k_{\max}$/Å^{-1} = (a) 2, (b) 0.5. The effect of electrolyte concentration in the non-aqueous phase: n_2, M = (1) 0.1, (2) 0.05, (3) 0.025.

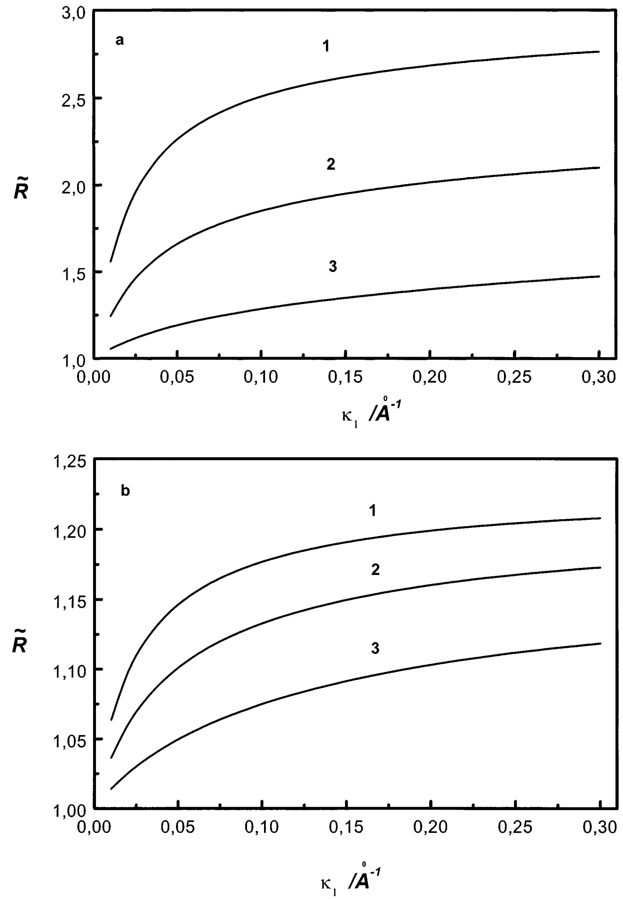

Fig. 5. Roughness function versus the Debye length in the aqueous phase at a fixed interfacial tension, $\gamma = 15$ dyn cm^{-1}, and a given concentration of non-aqueous phase, $n_2 = 0.1$ M. The upper wave-vector cutoff $k_{\rm max}$/Å^{-1} = (a) 2, (b) 0.5. The effect of dielectric constant of the non-aqueous solvent: ε_2 = (1) 4, (2) 10, (3) 30.

potential decreases with the increase of the electrolyte concentration. The reason for these effects is clear. The increase of the ionic concentration leads to a decrease of the thickness of the diffuse layer and as a result to an increase of the electric field acting on the interface. Obviously a fall in the interfacial tension leads to the enhancement of the field induced corrugation. Fig. 6b shows a comparison between results of calculations of $d^2_{\rm cw}$ within non-linear Poisson–Boltzmann theory and within the linear theory discussed above. We see that in the region of high electrode potentials, $E > 3kT/e$, the linear approximation underestimates the field induced enhancement of the corrugation.

The enhancement of the interfacial corrugation should manifest itself in the capacitance measurements. Fig. 7 shows the potential dependence of the roughness function, $\tilde{R} = C/C_{\rm GC}$, for several fixed values of the ionic concentration in the non-aqueous phase. We found that the double layer capacitance at the interface between two immiscible electrolytes is always larger than one prescribed by the 'flat-interface Gouy–Chapman theory', and its potential dependence is steeper than that of $C_{\rm GC}$. There are two different effects contributing to the enhancement of the capacitance: the influence of the interfacial corrugation on the distribution of the electric field at the boundary and the field induced increase of the corrugation. In order to clarify a relative role of these contributions we compared the results for $\tilde{R}$ obtained above with the potential dependence of the

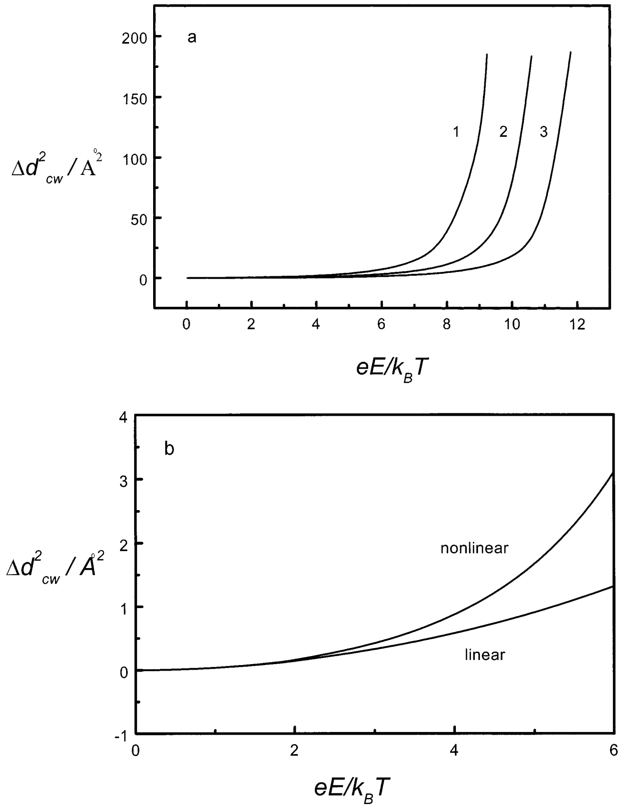

Fig. 6. The dependence of the mean square height of corrugations on the potential. (a) non-linear Poisson–Boltzman problem; $\varepsilon_2 = 10$, $\gamma = 30$ dyn cm^{-1}, κ_2/Å^{-1} = (1) 0.2; (2) 0.1; (3) 0.05; (b) the comparison between results of the calculations of $d^2_{\rm cw}$ within non-linear and linear approach; $\kappa_2 = 0.1$ Å^{-1}, $\varepsilon_2 = 10$, $\gamma = 30$ dyn cm^{-1}.

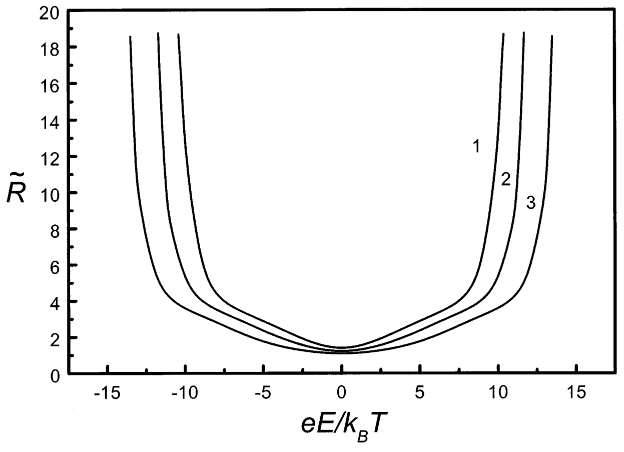

Fig. 7. Roughness function versus potential. $\varepsilon_2 = 10$, $\gamma = 30$ dyn cm^{-1}, κ_2/Å^{-1} = (1) 0.1; (2) 0.05; (3) 0.02.

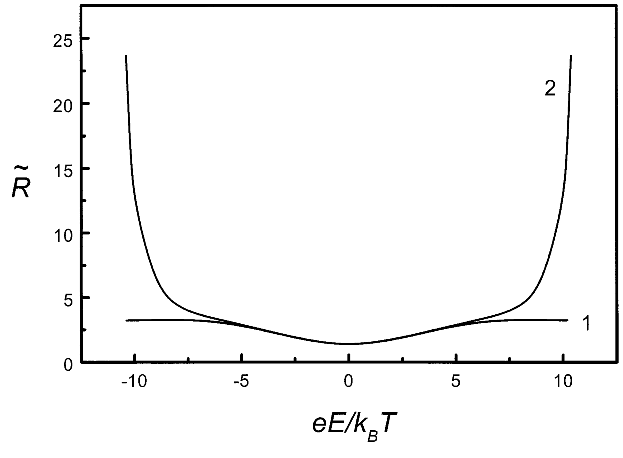

Fig. 8. Potential dependences of the roughness function for the fixed and the potential dependent correlation functions of interfacial corrugation. (1) $g(k, V=0)$; (2) $g(k, V)$; $\varepsilon_2 = 10$, $\gamma = 30$ dyn cm^{-1}, $\kappa_2 = 0.1$ Å^{-1}.

roughness function calculated for a fixed corrugation of the interface corresponding to the pzc (see Fig. 8). This comparison clearly demonstrates that in the region of low and moderate potentials, $E < 5kT/e$, the effect of the potential on the interfacial profile can be approximately neglected. However, in the region of high potentials, $E > 5kT/e$, the latter effect plays the main role.

The results obtained show that the linear response theory both for the amplitude of capillary waves and for the capacitance works eventually well for $V < 2$–$4k_BT/e$. At larger potential drops the non-linear theory predicts stronger effects than the linear theory. The large V regions, associated with the field induced enhancement of the amplitude of the capillary waves and the consequent enhancement of the double layer capacitance, will be in fact terminated by the field induced destruction of the interface [23]. Of course neither that critical range, nor the strongly enhanced but still stable regions cannot be quantitatively described by the formulae based on the perturbation theory, but the predicted trends seem to be correct.

4. Conclusions

4.1. Do we have a full and consistent theory of capillary waves at soft electrified interfaces?

The theory of capillary waves at electrified liquid | liquid interfaces, as presented above, is incomplete and in some aspects even internally inconsistent. Although it seems to be basically in line with existing experimental data, one must be aware of its factual status.

4.2. What is the nature of the electrolyte ions?

As we have mentioned in the Introduction, only the complete atomistic description of ions and molecules of the solvents can fully describe the smeared character of the interfacial region, treated above as the wavy sharp interface. However, before starting such a complicated enterprise, one may try to mimic the experimentally observed effect, by allowing the ions to distribute self-consistently between the two solvents. The basic Landau free energy should be modified then to incorporate such a parameter as the standard Gibbs energy of ion transfer between two solvents (e.g. from water to oil) [46]. Since this parameter is measurable to the accuracy of certain plausible assumptions, such an approach could directly trace the effect of the ion nature: relaxing the constraints on inter-penetration modifies the capacitance [7–9]. It is hard to envisage, prior the detailed analysis, whether the results of such modification would be in line with experimental trends, but it is obvious that the absolute values of the effect will not be negligible.

4.3. Can dynamics be ignored? Is the quasi-static theory consistent?

There is also a principle problem. Scattering experiments and simulations [12–14,24–26,45] show that the correlation function for capillary waves, which we used, works well up to wave–vectors of inverse molecular size. According to the capillary wave dispersion relation (Eq. (9)), this corresponds to formally very high frequencies (up to 10^{12} s^{-1}), but with even higher decay decrements. Obviously, the ionic distribution in electrolyte cannot respond to the momentary values of the surface corrugation, which changes with the frequencies exceeding the characteristic frequency of the double layer response. The latter will impose an adiabatic cut-off frequency, ω_*. For the Fourier-components of the fluctuations with the frequency, $\omega > \omega_*$, the double layer will see only the time averaged profile, which corresponds to the flat interface. Therefore, such a high frequency domain of the capillary wave spectrum cannot influence the capacitance. What is the nature of the cut-off frequency? A first reaction would be to put ω_* equal to the inverse Debye relaxation time of the double layer, $\omega_D \approx D\{\min(\kappa_1, \kappa_2)\}^2$, where D is the diffusion coefficient for ions in the solution. However, our calculations presented above suggest that ω_* can be much higher than ω_D. Indeed, if we rest our estimates on simple scaling arguments, we cannot ignore that in the theory of the roughness effect on capacitance a newlength scale comes out, introduced by surface corrugations. This is, $[(\min(\kappa_1, \kappa_2))^2 + k_{\max}^2]^{-1/2}$, rather than simply $[\min(\kappa_1, \kappa_1)]^{-1/2}$. Based on this length scale we get $\omega_* = D[(\min(\kappa_1, \kappa_2))^2 + k_{\max}^2]$. Taking into account that the upper wave-vector cut-off $k_{\max}$ is of the order of 1 Å we see that such a cut-off is much higher than ω_D, being of the order of 10^{11} s^{-1}. As a solid estimate cannot be made a priori detailed dynamic theory, we can assert that the cut-off frequency should lie in the interval between these two limits.

Now the question arises, how does the introduction of the frequency cut-off modify the height–height correlation function of fluctuations seen by the double layer? In order to answer this question we have to consider a spectrum of interfacial fluctuations $S(k, \omega)$ defined by the equation [47]:

$$(2\pi)^3\delta(\omega-\omega')\delta^2(\boldsymbol{k}-\boldsymbol{k}')S(\boldsymbol{k}, \omega) = <\xi(\boldsymbol{k}, \omega)\xi^*(\boldsymbol{k}', \omega')> \quad (44)$$

where

$$\xi(\boldsymbol{k}, \omega) = \int \mathrm{d}\boldsymbol{R}\mathrm{d}t \, \exp(-\mathrm{i}\boldsymbol{kR} - \mathrm{i}\omega t)\xi(\boldsymbol{R}, t) \quad (45)$$

and $\xi(\boldsymbol{R}, t)$ is the time-dependent fluctuation of the interface. The spectrum of the capillary wave fluctuations is described by the following equation [47]

$$S(\boldsymbol{k}, \omega) = \frac{4k_{\mathrm{B}}T\Delta(k)k/(\rho_1 + \rho_2)}{[\omega^2 - \omega_{\mathrm{c}}^2(k)]^2 + 4\Delta^2(k)\omega^2} \quad (46)$$

Then the height–height correlation function $g_*(\boldsymbol{k})$, which determines the effect of capillary fluctuations on the capacitance, can be defined as

$$g^*(\boldsymbol{k}) = \int_0^{\omega_*} \frac{\mathrm{d}\omega}{\pi} S(\boldsymbol{k}, \omega) \quad (47)$$

For $\omega_* = \infty$, Eq. (47) reduces to the full correlation function $g(\boldsymbol{k})$, given by Eq. (7). An expression for a truncated correlation function $g_*(\boldsymbol{k})$ which results from Eqs. (46) and (47) is presented in the Appendix B. In order to reveal the effect of the cut-off frequency on the double layer capacitance we calculated the roughness function $\tilde{R}_*(\kappa_1, \kappa_2, V = 0)$ via Eq. (43) with the truncated correlation function $g_*(\boldsymbol{k})$. As the exact value of ω_* is unknown, we vary it in the range corresponding to the above mentioned two limits.

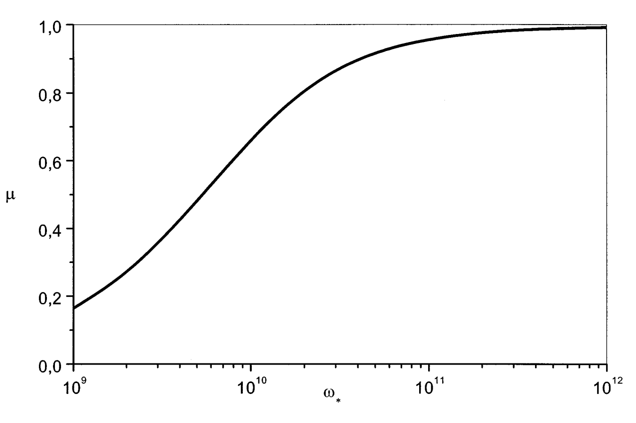

Fig. 9. The influence of dynamical effects on the roughness function, $\mu = \{\tilde{R}_*(\kappa_1, \kappa_2, V = 0) - 1\}/\{\tilde{R}(\kappa_1, \kappa_2, V = 0) - 1\}$ versus the cut-off frequency ω_*. $\eta_{1,2} = 1$cP, $\gamma = 10$ dyn cm^{-1}, $\rho_{1,2} = 1$ g cm^{-3}, $\kappa_{1,2} = 0.01$ Å^{-1}, $\varepsilon_1 = 80$, $\varepsilon_2 = 10$, $k_{\max} = 1$ Å.

Fig. 9 demonstrates the effect of ω_* showing $\mu = (\tilde{R}_* - 1)/(\tilde{R} - 1)$ as a function of the cut-off frequency for fixed values of the Debye lengths in the solutions. We see that the modified roughness function $\tilde{R}_*(\kappa_1, \kappa_2, V = 0)$ approaches the roughness function given by Eq. (43) with a increase of the cut-off frequency. Already for $\omega_* = 10^{11}$ s^{-1}, the dynamical effect is negligible and the results of the present work can be used without any modifications. As we have already mentioned above, the value $\omega_* = 10^{11}$ s^{-1} is not that unreasonable if we rely on the scaling estimates.

The estimates above were performed for the pzc case, where the effect of the cut-off is strongest. For polarized interfaces, the role of the dynamic cut-off will be diminished, since the integral for the roughness function converges at smaller k and, furthermore, the electric field lowers the frequencies of capillary waves.

Of course these estimates cannot replace a more detailed, dynamic variant of the theory. Whether it will only specify a self-consistent value of the dynamic cut-off, or do something unexpected, with a considerable effect on the capacitance, we do not know. Future investigations must give the answer to this question.

Acknowledgements

The authors are grateful to Ilan Benjamin, Bob Samec and Sasha Volkov for useful discussions and consultations. The financial support of this work by DAAD and the Bureau of Public Relations, International and Industrial Affairs of the Research Center Juelich is greatly appreciated.

Appendix A

In order to determine the first non-vanishing correction to the free energy caused by interfacial corrugation, we must find $\psi_2(r)$ up to the second order in the root mean square height of the corrugation, $d_{\mathrm{cw}} = (<\xi^2>)^{1/2}$. For this purpose we expand the potential in powers of h,

$$\psi_2(z, R) = \psi_2^{(0)}(z, R) + \psi_2^{(1)}(z, R) + \psi_2^{(2)}(z, R) \quad (\mathrm{A1})$$

Substituting the expansion (Eq. (A1)) into Eqs. (11)–(13), we obtain the following equations for the free energy, F, and for the charge in the second phase, Q

$$
\begin{aligned}
&F[\xi(R), V] \\
&= F_0 + \frac{1}{2}\int \mathrm{d}R\gamma[(\nabla\xi(R))^2 + k_{\mathrm{gr}}^2\xi^2(R)] \\
&\quad - \frac{2n_2^0k_{\mathrm{B}}T}{\kappa_2^2}\int \mathrm{d}R\left[\left(\psi_2^{(0)}\frac{\partial\psi_2^{(0)}}{\partial z} + \psi_2^{(0)}\frac{\partial\psi_2^{(1)}}{\partial n}\right)_{z=\xi(R)}\right. \\
&\quad \left. + \left(\psi_2^{(0)}\frac{\partial\psi_2^{(2)}}{\partial z} + \frac{1}{2}\psi_2^{(1)}\frac{\partial\psi_2^{(1)}}{\partial z}\right)_{z=0}\right] \\
&\quad - \frac{n_2^0k_{\mathrm{B}}T}{\kappa_2^2}\int \mathrm{d}R\int_{\xi(R)}^{\infty}\mathrm{d}z\left[\left(\frac{\partial\psi_2^{(0)}}{\partial z}\right)^2\right. \\
&\quad \left. - 2\kappa_2^2(1-\cosh((\psi_2^{(0)}))\right] + VQ \qquad \text{(A2)}
\end{aligned}
$$

$$
\begin{aligned}
Q &= \int_{\mathrm{interface}} \mathrm{d}S\sigma(R) \\
&= -\frac{\varepsilon_2k_{\mathrm{B}}T}{4\pi e}\int \mathrm{d}R\left[\frac{\partial\psi_2^{(0)}}{\partial z} + \frac{\partial\psi_2^{(1)}}{\partial z} + \frac{\partial\psi_2^{(2)}}{\partial z}\right. \\
&\quad \left. - \frac{\partial\xi(R)}{\partial R}\frac{\partial}{\partial R}(\psi_2^{(0)} + \psi_2^{(1)})\right]_{z=\xi(R)} \qquad \text{(A3)}
\end{aligned}
$$

Here $\sigma(R)$ is the local density of the surface charge on one side of the interface, which is related to the potential as

$$\frac{4\pi\sigma(R)}{\varepsilon_2} = \frac{\partial\phi_2(R, z=\xi(R))}{\partial n} \qquad \text{(A4)}$$

The solutions of non-linear Poisson–Boltzmann equation (Eq. (15)) for functions $\psi_2^{(0,1,2)}$ have been found along the lines of Ref. [36], where we solved the non-linear problem within the context of a double layer capacitance at a rough metal | electrolyte interface. As a result we get

$$\psi^{(0)}(z, R) \equiv \psi^{(0)}(z) = 4\arctan\{\exp[-\kappa(z+z_0)]\} \qquad \text{(A5)}$$

$$
\begin{aligned}
\psi_2^{(1)}(z, k) &= A(k)\exp[-q_2(k)(z+z_0)] \\
&\quad [\kappa_2\coth(\kappa_2(z+z_0)) + q_2(k)] \qquad \text{(A6)}
\end{aligned}
$$

$$
\begin{aligned}
&\psi_2^{(2)}(z, 0) \\
&= B_0\kappa_2^2\exp[-\kappa_2(z+z_0)][\coth(\kappa_2(z+z_0)) + 1] \\
&\quad + \frac{\kappa_2^4}{\sinh[\kappa_2(z+z_0)]\sinh^2(\kappa_2z_0)} \\
&\quad \times \int\frac{\mathrm{d}k}{(2\pi)^2}\xi(k)\xi(-k) \\
&\quad \frac{\exp(-2q_2(k)z)[\coth(\kappa_2(z+z_0)) + \kappa_2/q_2(k)]}{(\kappa_2\coth(\kappa_2z_0) + q_2(k))^2} \qquad \text{(A7)}
\end{aligned}
$$

where z_0 is given by

$$\arctan\{\exp[-\kappa_2z_0]\} = V/4 \qquad \text{(A8)}$$

$$A(k) = \frac{2\kappa_2\xi(k)\exp(q_2(k)z_0)}{\sinh(\kappa_2z_0)[\kappa_2\coth(\kappa_2z_0) + q_2(k)]} \qquad \text{(A9)}$$

and

$$
\begin{aligned}
B_0 &= \frac{\exp(\kappa_2z_0)}{\sinh(\kappa_2z_0)[\coth(\kappa_2z_0)+1]}\int\frac{\mathrm{d}k}{(2\pi)^2}\xi(k)\xi(-k) \\
&\quad \times\left[\frac{2q_2(k)}{\kappa_2} - \coth(\kappa_2z_0)\right. \\
&\quad + \frac{1}{\sinh^2(\kappa_2z_0)[\coth(\kappa_2z_0) + q_2(k)/\kappa_2]} \\
&\quad \left.\left(1 + \frac{k^2}{\kappa_2q_2(k)\coth(\kappa_2z_0) + q_2^2(k)}\right)\right] \qquad \text{(A10)}
\end{aligned}
$$

Substitution of the solutions (Eqs. (A5), (A6) and (A7) into Eqs. (A2) and (A3) leads to Eqs. (24) and (30) for the free energy functional and for the interfacial charge, which are presented in the text.

Appendix B

The truncated height–height correlation function $g_*(k)$, given by Eqs. (46) and (47), can be calculated analytically. In the region of large wave-vectors, which gives the main contribution to the corrugation-induced correction to the capacitance, the correlation function $g_*(k)$ can be written in the form

$$
\begin{aligned}
&g_*(k) \\
&= \frac{4k_{\mathrm{B}}T\Delta(k)k}{\pi(\rho_1+\rho_2)h(k)}\left[\frac{1}{\sqrt{f(k)}}\arctan\frac{\omega_*}{\sqrt{f(k)}}\right. \\
&\quad \left. - \frac{1}{\sqrt{p(k)}}\arctan\frac{\omega_*}{\sqrt{p(k)}}\right] \qquad \text{(B1)}
\end{aligned}
$$

where

$$
\begin{aligned}
h(k) &= 4\Delta(k)[\Delta^2(k) - \omega_{\mathrm{c}}^2(k)]^{1/2} \\
f(k) &= \{\Delta(k) - [\Delta^2(k) - \omega_{\mathrm{c}}^2(k)]^{1/2}\}^2 \\
p(k) &= \{\Delta(k) + [\Delta^2(k) - \omega_{\mathrm{c}}^2(k)]^{1/2}\}^2 \qquad \text{(B2)}
\end{aligned}
$$

It should be noted that in the region of wave-vectors relevant for the calculations of the capacitance the damping coefficient, $\Delta(k)$, of the capillary waves is much larger than their frequency, $\omega_{\mathrm{c}}(k)$.

For the cut-off frequency ω_*, which is much higher than $\omega_{\mathrm{c}}(k)$ and $\Delta(k)$, Eq. (B1) reduces to Eq. (7), i.e. the full expression for the height–height correlation function. However for realistic values of the parameters, γ, $\eta_{1,2}$, and $\rho_{1,2}$, and $k \approx k_{\max}$ the cut-off frequency ω_* is smaller than $\omega_{\mathrm{c}}(k)$and $\Delta(k)$. Under the conditions $\omega_* \gg \Delta$, $\omega_{\mathrm{c}}^2/\Delta$ the modified correlation function $g_*(k)$ can be approximated by the equation

$$g_*(k) \approx \frac{2}{\pi}g(k)\frac{\omega_*(\eta_1+\eta_2)}{\gamma k} \qquad \text{(B3)}$$

Thus we see that accounting for the dynamical effects changes not only the absolute value of the correlation function, but it also modifies its dependence on the wave-vector. Eq. (B3) shows that for $\eta_{1,2} \approx 1$cP, $\gamma = 30$ dyn cm^{-1} and $k \approx k_{\max} \approx 1$ Å the correlation function

$g_*(\boldsymbol{k})$is smaller than $g(k)$ for $\omega_* < 10^{11}$ s^{-1} and approaches $g(\boldsymbol{k})$ for $\omega_* \approx 10^{11}$ s^{-1}. This conclusion is in agreement with the results of calculations presented in Fig. 9, which shows that for $\omega_* \geq 10^{11}$ s^{-1} the dynamical effects do not influence the corrugation-induced corrections to the capacitance.

References

[1] M. Daoud, C.E. Williams (Eds.), Soft Matter Physics, Springer, Berlin, 1999.
[2] J.C. Rowlinson, B. Widom, Molecular Theory of Capillarity, Clarendon, Oxford, 1982.
[3] H.H. Girault, in: J.O'M. Bockris, et al. (Eds.), Modern Aspects of Electrochemistry, vol. 25, Plenum, New York, 1993, p. 1.
[4] H.H.J. Girault, D.H. Schiffrin, in: A.J. Bard (Ed.), Electroanalytical Chemistry, vol. 15, Marcel Dekker, New York, 1989, p. 1.
[5] A.G. Volkov, D.W. Deamer, D.I. Tanelian, V.S. Markin, Liquid Interfaces in Chemistry and Biology, Wiley, New York, 1998, p. 551.
[6] C.A. Croxton, Statistical Mechanics of the Liquid Surface, Wiley, New York, 1980.
[7] C.M. Pereira, W. Schmickler, F. Silva, M.J. Sousa, Chem. Phys. Lett. 268 (1997) 13.
[8] C.M. Pereira, W. Schmickler, F. Silva, M.J. Sousa, J. Electroanal. Chem. 436 (1997) 9.
[9] T. Huber, O. Pecina, W. Schmickler, J. Electroanal. Chem. 467 (1999) 203.
[10] M.P. Gelfand, M.E. Fisher, Physica A 166 (1990) 1.
[11] F. Buff, R. Lovett, F. Stillinger, Phys. Rev. Lett. 15 (1965) 621.
[12] I. Benjamin, in: D.L. Thompson (Ed.), Modern Methods for Multidimensional Dynamics Computations in Chemistry, World Scientific, Singapore, 1998, p. 101.
[13] K.J. Schweighofer, I. Benjamin, J. Electroanal. Chem. 391 (1995) 1.
[14] B.M. Ocko, X.Z. Wu, E.B. Sirota, S.K. Sinha, M. Deutsch, Phys. Rev. Lett. 2 (1994) 242.
[15] Z. Samec, J. Langmaier, A. Trojanek, J. Electroanal. Chem. 463 (1999) 232.
[16] D. Savignac, P. Leiderer, Phys. Rev. Lett. 49 (1982) 1869.
[17] J.I. Frenkel, Phys. Z. Sowjet Union 8 (1935) 675.
[18] L. Tonk, Phys. Rev. 48 (1935) 562.
[19] G.I. Tayler, A.D. McEwan, J. Fluid Mech. 22 (1965) 1.
[20] L.P. Gorkov, D.M. Chernikova, JETP Lett. 18 (1973) 68.
[21] K. Mima, H. Ikezi, A. Hasegawa, Phys. Rev. B14 (1976) 3953.
[22] M. Wanner, P. Leiderer, Phys. Rev. Lett. 42 (1979) 315.
[23] A. Onuki, Physica A 217 (1995) 38.
[24] D. Beaglehole, Phys. Rev. Lett. 58 (1987) 1434.
[25] L.T. Lee, D. Langevin, J. Meunier, K. Wong, B. Cabane, Prog. Colloid. Polym. Sci. 81 (1990) 209.
[26] L.T. Lee, D. Langevin, B. Farnoux, Phys. Rev. Lett. 67 (1991) 2678.
[27] S.A. Safran, Statistical Thermodynamics of Surfaces. Interfaces and Membranes, Addison-Wesley, Reading, MA, 1994.
[28] J.D. Weeks, J. Chem. Phys. 67 (1977) 3106.
[29] R. Evans, Adv. Phys. 28 (1979) 143.
[30] Z.-H. Zhang, I. Tsuyumoto, S. Takashi, T. Kitamori, T. Sawada, J. Phys. Chem. A 101 (1997) 4163.
[31] Z.-H. Zhang, I. Tsuyumoto, T. Kitamori, T. Sawada, J. Phys. Chem. B 102 (1998) 10284.
[32] L.I. Daikhin, A.A. Kornyshev, M. Urbakh, Chem. Phys. Lett. 309 (1999) 137.
[33] L.I. Daikhin, A.A. Kornyshev, M. Urbakh, Electrochim. Acta 45 (1999) 685.
[34] L.I. Daikhin, A.A. Kornyshev, M. Urbakh, in preparation.
[35] L.D. Landau, E.M. Lifshitz, Electrodynamics of Continuous Media, Pergamon, Oxford, 1984, p. 8.
[36] L.I. Daikhin, A.A. Kornyshev, M. Urbakh, J. Chem. Phys. 108 (1998) 1715.
[37] P. Delahey, Double Layer and Electrode Kinetics, Interscience, New York, 1965.
[38] S.L. Carnie, G.M. Torrie, Adv. Chem. Phys. 56 (1984) 141.
[39] L. Blum, Adv. Chem. Phys. 78 (1990) 171.
[40] O. Pecina, J.P. Badiali, Phys. Rev. E 58 (1998) 6041.
[41] Z. Samec, Chem. Rev. 88 (1988) 617.
[42] Y. Chang, V.J. Cunnane, L. Murtomaki, D.J. Schiffrin, J. Chem. Soc. Faraday Trans. 87 (1991) 107.
[43] C.M. Pereira, A. Martins, M. Rochas, A.J. Silva, A.F. Silva, J. Chem. Soc. Faraday Trans. 90 (1994) 143.
[44] Wandlowski, K. Holub, V. Marecek, Z. Samec, Electrochim. Acta 40 (1995) 887.
[45] M.K. Sanyal, S.K. Sinha, K.G. Huang, B.M. Ocko, Phys. Rev. Lett. 66 (1991) 628.
[46] A.A. Kornyshev, A.G. Volkov, J. Electroanal. Chem. 180 (1984) 363.
[47] R.C. Desai, M. Grant, in: C.A. Croxton (Ed.), Fluid Interfacial Phenomena, Wiley, New York, 1986, p. 135.